LA-UR-21-29705
Approved for public release; distribution is unlimited.

Title: PHOENIX Electrostatic Design

Author(s): Watson, Scott Avery
Winch, Mary Jane (Mary Jane)
Sorensen, Eric Byron
Romero, Richard Chris
Misurek, Lauren Ashley
Platts, David
McEliggot, Patrick

Intended for: Report

Issued: 2021-09-30

PHOENIX Electrostatic Design

LA-UR-XYZPDQ

by

Scott A. Watson, Group A-3 Applied Technology;

Eric Sorensen, Nicola Winch, Lauren Misurek, Group NEN-2 Advanced Nuclear Technology;

Chris Romero, Group E-1Mechanical and Thermal Engineering;

and

David Platts, Group MPA-Q Material Physics and Applications

Los Alamos National Laboratory

and

Midshipman Patrick E. McElligott, United States Navy,

September, 2021

Abstract

PHOENIX (Portable, High-efficiency, Optimal ENergy Imaging X-rays) is a quasi-DC, electrostatic, vacuum-diode designed as a portable x-ray source with national defense and commercial applications. The patent-pending PHOENIX concept combines a megavoltage, Cockroft-Walton voltage multiplier[1] with a Van de-Graaff electrostatic charge-storage dome to create a vacuum-diode suitable for x-ray production. Naturally this structure must minimize internal electric fields to reduce electrical breakdown while simultaneously reducing size and weight to enhance portability. In this paper we describe the optimization process and model results obtained using the COMSOL multi-physics code. We describe three models: a prototype model (see Figures1-6) built to demonstrate the PHOENIX concept as part of Laboratory Directed Research and Development (LDRD) Mission Foundation Research (MFR) Phase-I , a "back-of-the-envelope" design (Figures 7-11) used as a starting point for further COMSOL optimization, and finally, the optimized geometry (Figures 12-17) implemented in the MFR Phase-II. In all cases compromises resulting from cost, schedule, and manufacturing constraints were taken into account as the design progressed.

Introduction

Despite more than a century of development of electrostatic "influence machines", high-voltage, DC diodes remain relatively rare. Modern examples are primarily used as photo-injectors for free-electron-lasers - for example at Thomas Jefferson Lab[2] and in Japan[3]. While our work with electrostatic generators like MEXRAY[4] and work with plasma-etched electrodes[5] indicates that DC electric fields as high as 30MV/m can be sustained in a vacuum on large, epoxy-coated capacitor plates, an electric field threshold of 10 MV/m DC is more widely accepted[6,7] for mirror polished metals with large gaps[8].

Taking 10MV/m a design goal, our optimization was also subject to the constraint that the initial, 1MV diode must fit within a 24" diameter cylindrical vessel (aka "the pickle barrel" shown in Figure 1) and that the follow-on, 2MV hydrotesting design must fit within a 48" cylindrical diameter vessel. Finally, we sought to mimimize the field strength near the cathode triple-point and near both plastic and metal connectors.

The electrostatic field-strength is related to the diode geometry, the voltages applied and the materials within the device. These are modeled using the COMSOL multiphysics code[9] and evaluated with a "fine" mesh to seek minimum electric fields given other constraints of size, weight, and volume. In our studies, 2-D axisymmetric (coaxial) geometries were tested within the same basic structure consisting of: a vacuum vessel, a Van de Graaff dome, and 10 field shrouds each connected to a voltage multiplier circuit within a tapered epoxy insulator similar to the prototype shown in Figure 3.

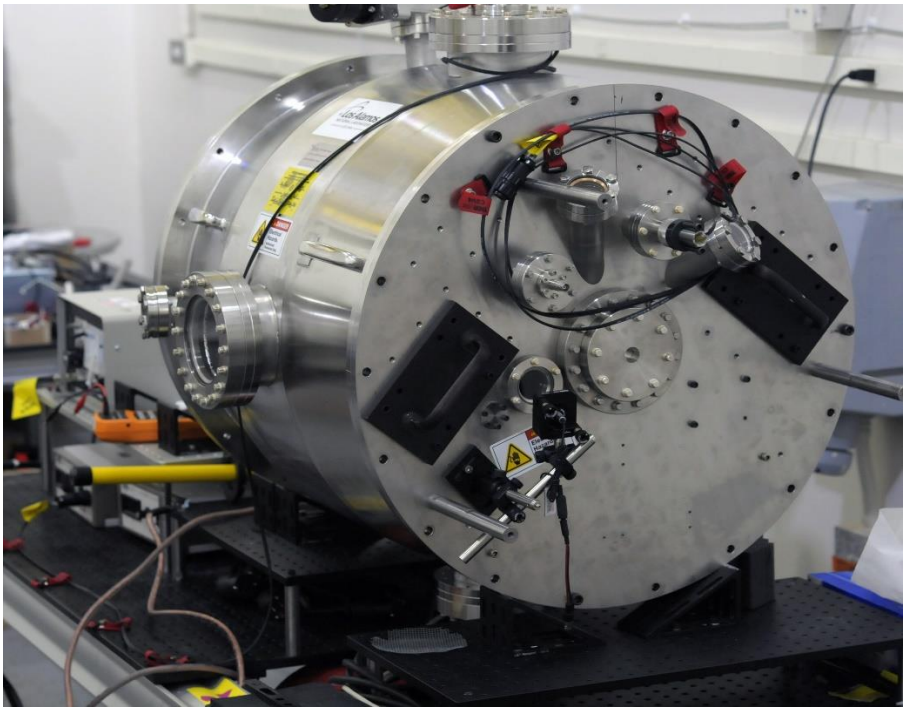

Figure 1 – 24” diam., 24” long, “pickle-barrel” vacuum chamber used for LDRD, MFR studies

Figure 2 – MFR Phase I PHOENIX cutaway showing Cockroft-Walton modules (left) and Van de Graaff “dome”, (right)

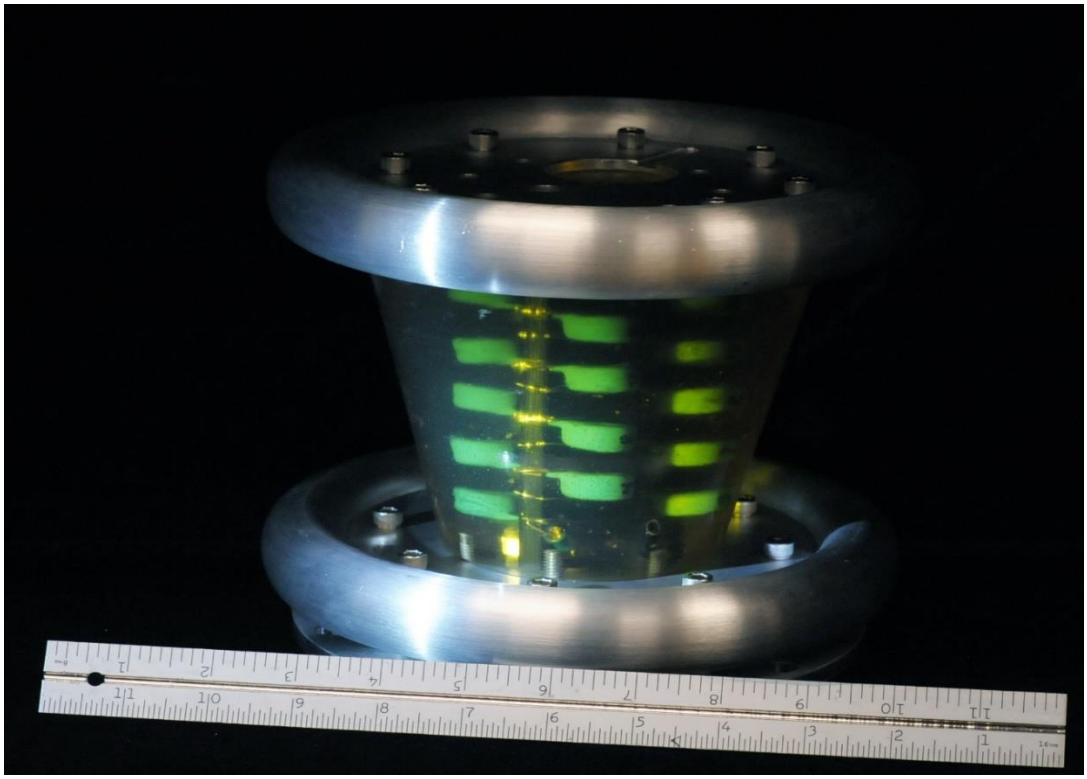

Figure 3 – PHOENIX MFR Prototype Cockroft-Walton module

PHASE I MFR Design

For completeness, we evaluated the electrostatics of the PHASE I MFR design shown if Figures 1-3. In part due to the limited time and budget allocated to that effort, this device was quite crude. Nonetheless, it did successfully demonstrate the unique combination of a Cockroft-Walton and Van de Graaff at 600kV – which was the goal of the MFR.

Our experimental studies also indicated significant field-emission from both the cathode shroud and the aluminum "corona[1]" rings as diagnosed by a Geiger counter and special-purpose field probes. Initially these rings were unpolished and had significant field emission. Subsequent versions were hand-polished to a mirror-finish with much reduced field-emission. These were conditioned to approximately 600kV (as verified by an ORTEC, high-purity germanium, gamma-spectrometer).

Taking Figure 4 as a representative example of the electric fields present in our Phase I design and testing, we observe that peak fields of 30MV/m are expected at the full, 1MV charge voltage (see Figures 4-5). Since we were only able to demonstrate operation at 600kV, we witnessed fields as high as 18MV/m on polished aluminum – again, with significant field emission.

[1] Recognizing that there isn't any true corona loss in our system, we adopted the term "corona" ring here because the actual components used were, in fact, aluminum high-voltage corona rings adapted from high-voltage power distribution systems.

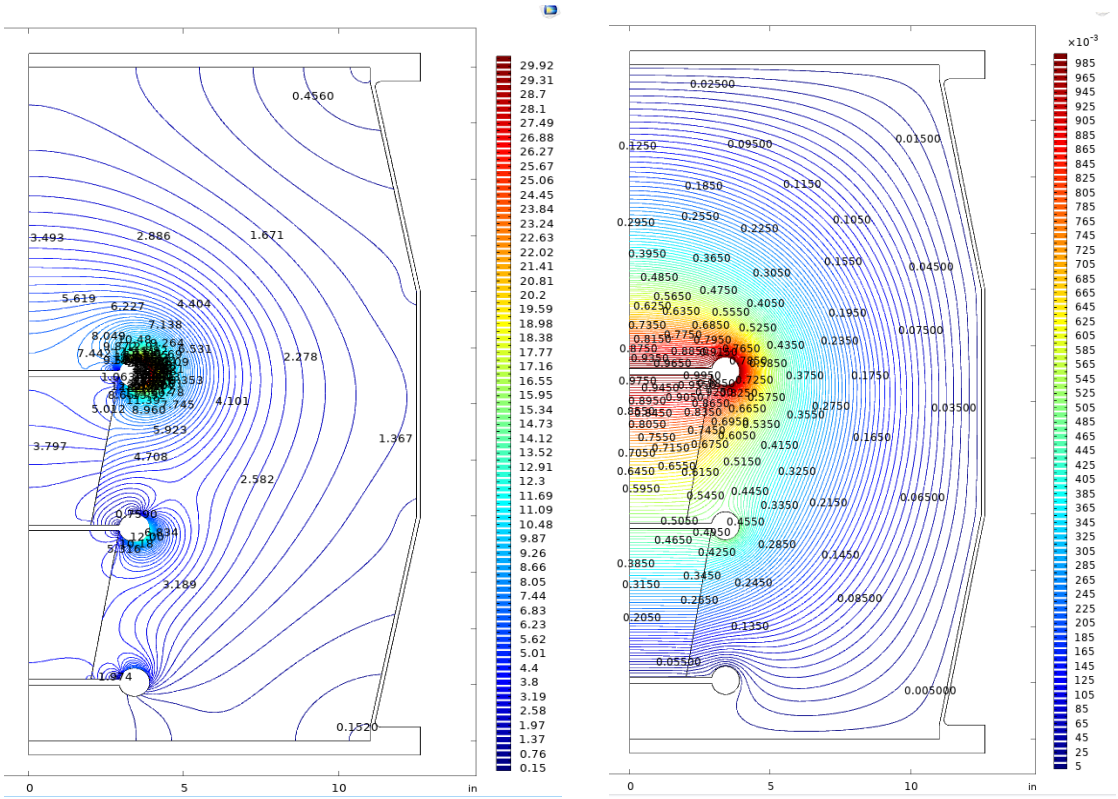

Figure 4: Cutaway view of PHOENIX PHASE I prototype. The COMSOL model shows ~30MV/m peak electric fields (left) and the corresponding equipotential lines (right).

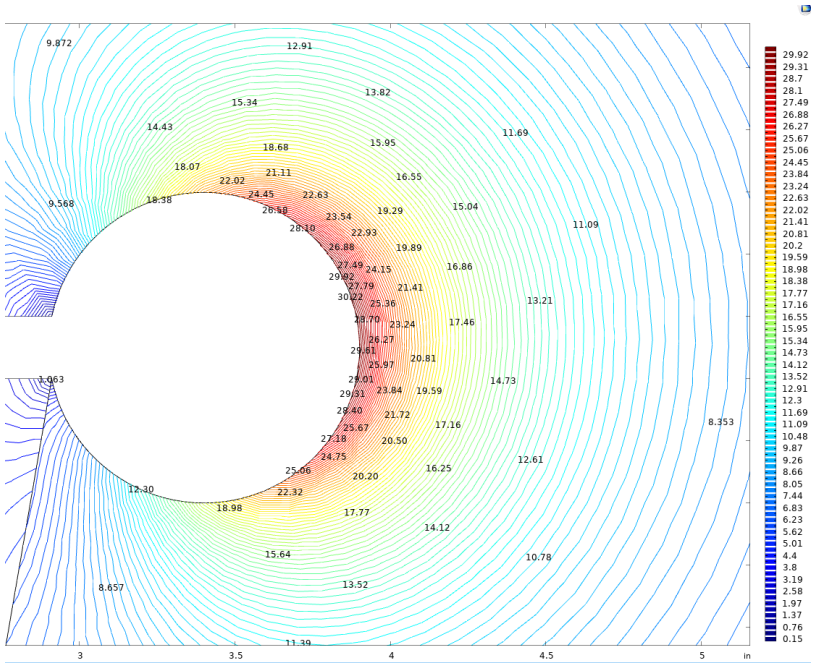

Figure 5: Blow-up view of PHASE I prototype shroud with electric field lines. Electric fields peak at ~30 MV/m at the rightmost point of the shroud.

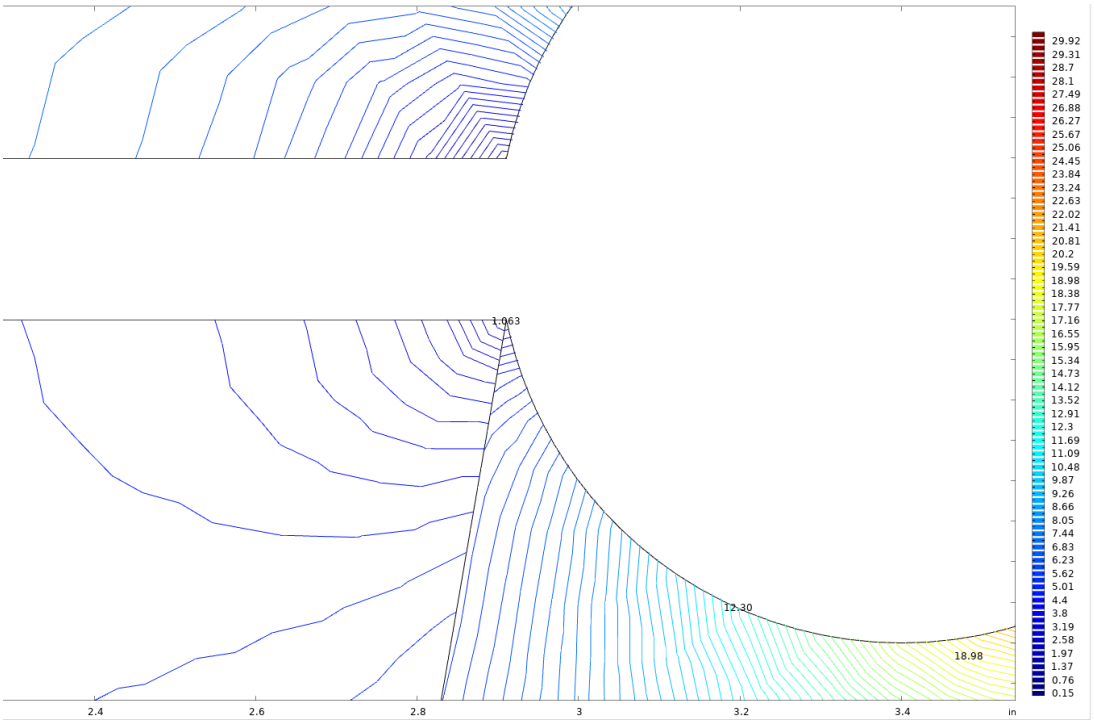

Figure 6: Blow-up view of the PHASE I design's cathode triple point with electric field lines. Electric field strength of approximately 6 MV/m in this region @ 1MV operation.

Finally, our calculations indicate that the cathode-triple-point junction has fields as high as 6MV/m (4MV/m @ 600kV operation) as shown in Figure 6.

Taking this information forward into PHASE II, it was clear that a more sophisticated field shroud would be required to accomplish our ultimate goals. In addition, it was desided to use either polished stainless steel or titanium shrouds as these are more common in the literature and generally have better performance often attributed to their higher work function and "refractory" nature.

PHASE II Design

Two geometries (shown in Figure 7) were used to obtain an initial estimate of field stresses in our design. The first geometry is of two, nested, concentric spheres, and the second is of a simple, coaxial-line with a charged interior conductor and a grounded exterior conductor.

Gauss' law can be used to find analytic solutions for the electric fields in these simple geometries, which represent a rough approximation to the geometry present in our situation. These analytic geometries were chosen to gain insights into the problem space.

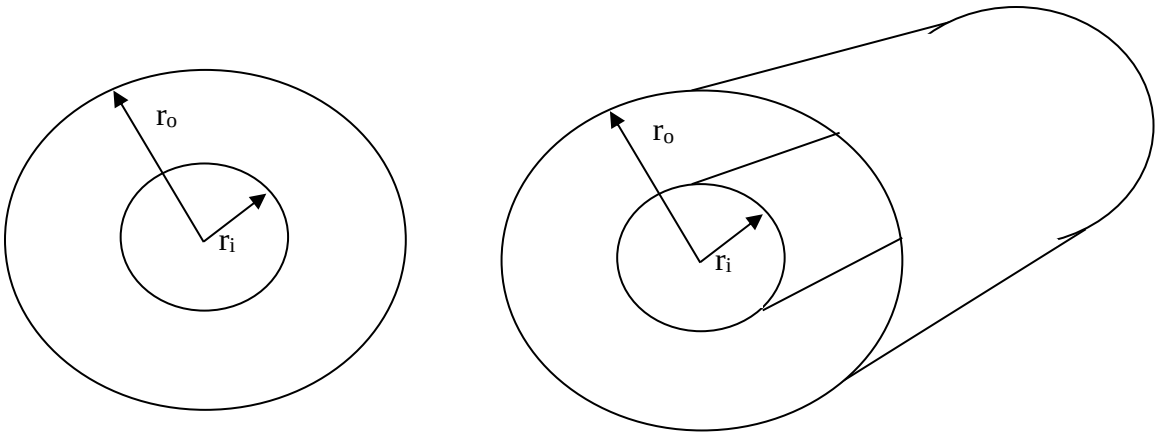

Figure 7 – Concentric sphere and coaxial geometries

Let us start by recognizing that the capacitance, C, between the two concentric spheres enclosing a vacuum dielectric is given by:

$$C = \frac{4\pi\varepsilon_o r_o r_i}{r_o - r_i} \tag{1}$$

We further note that if the inner sphere is has a charge, Q, on it, the voltage, V, between the two spheres is given by:

$$V = \frac{Q}{C} \tag{2}$$

The analytic expression for the radial electric field, E_r, present in the region, $r_i<r<r_o$, is given by:

$$\overrightarrow{E_r} = \frac{Q}{4\pi\varepsilon_o r^2} \tag{3}$$

By substitution, we have:

$$\overrightarrow{E_r} = \frac{r_i r_o V}{(r_o - r_i) r^2} \tag{4}$$

The peak electric field occurs on the surface of the inner sphere when $r=r_i$, or:

$$\vec{E}_r = \frac{V r_o}{(r_o - r_i) r_i} \tag{5}$$

To minimize this field with respect to the inner radius, we set the partial derivative with respect r_i to zero or:

$$\frac{\partial \vec{E}_r}{\partial r_i} = \frac{V r_o (r_o - 2r_i)}{r_i^2 (r_o - r_i)^2} = 0 \rightarrow r_i = \frac{r_o}{2} \tag{6}$$

This analysis gives us basic ***Design rule #1: for a fixed voltage, the peak electric field between concentric spheres is minimized for $r_i=r_o/2$***. Consequently, we start our design effort for the Van de Graaff dome with a dome radius set to half the radius of our barrel, or 6".

The simplified analytic description for concentric "cylindrical" parts is similar, but with modified mathematical details. In that latter case the radial electric field, E_r ($r_i<r<r_o$) is given by:

$$\vec{E}_r = \frac{V}{r ln\left(\frac{r_o}{r_i}\right)} \tag{7}$$

Setting the partial derivative with respect to the inner radius, r_i, to zero, at $r=r_i$ (where the field is maximum) gives:

$$\frac{\partial \vec{E}_r}{\partial r_i} = \frac{-ln\left(\frac{r_o}{r_i}\right)+r_o ln\left(\frac{r_o}{r_i}\right)}{\frac{r_o}{r_i}\left(r_i ln\left(\frac{r_o}{r_i}\right)\right)^2} = 0 \rightarrow ln\left(\frac{r_o}{r_i}\right) = 0 \ \rightarrow \frac{r_o}{r_i} = e \tag{8}$$

giving us ***Design rule #2: for a fixed voltage, the peak electric field between two coaxial cylinders is minimized when $r_o/r_i=e$***. Consequently, we start our design effort with the inner, field shrouds having a radius of 4.1".

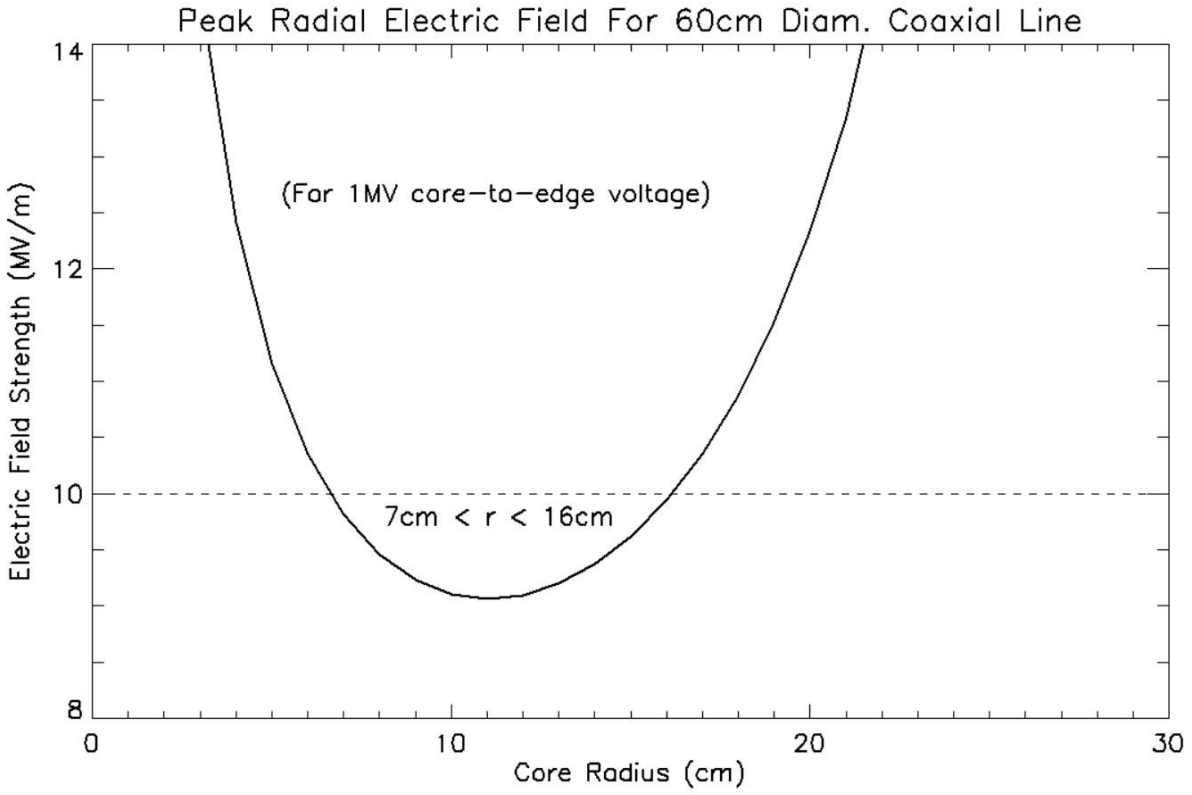

Figure 8 – Peak radial electric field for 60cm diameter (24") coaxial line. Note that the minimum field occurs when $r_i=r_o/e$ =11cm.

An example of this behavior for a 60cm (24”) diameter coaxial line, with a 1MV voltage from core to edge is shown in Figure 8. Note that the minimum (peak) field is about 9MV//m and occurs over a somewhat broad minium radius (+/- 2cm).

The peak electric fields calculated with COMSOL are shown in Figure 9 below and are somewhat higher than our analytic approximations – perhaps justifying the need for more careful optimization.

Figures 10 and 11 illustrate the fields around the module shrouds and triple-points respectively.

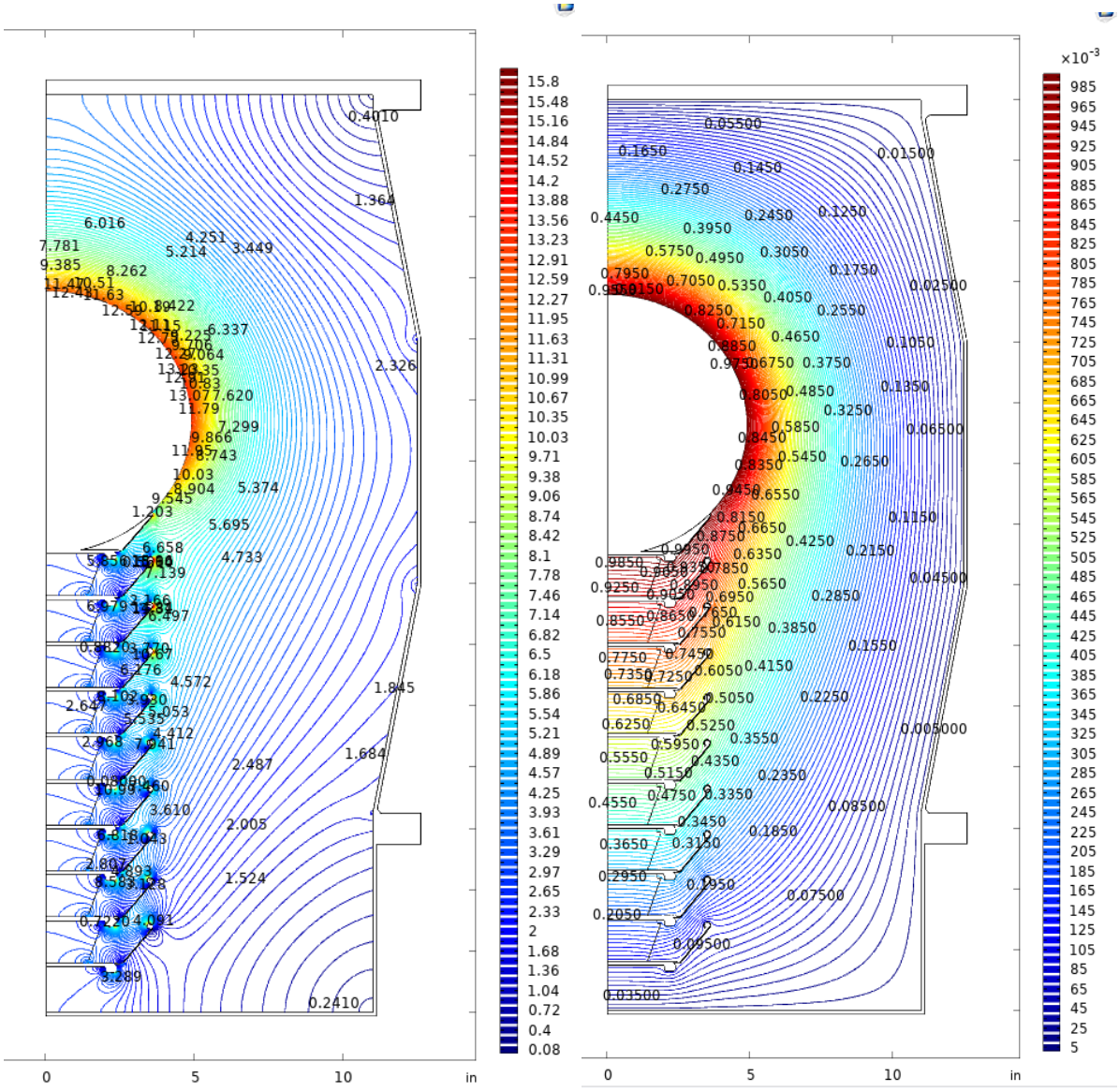

Figure 9: Cutaway view of the second-generation COMSOL model showing electric field lines (left) with a peak electric field of 16 MV/m, and equipotential lines (right).

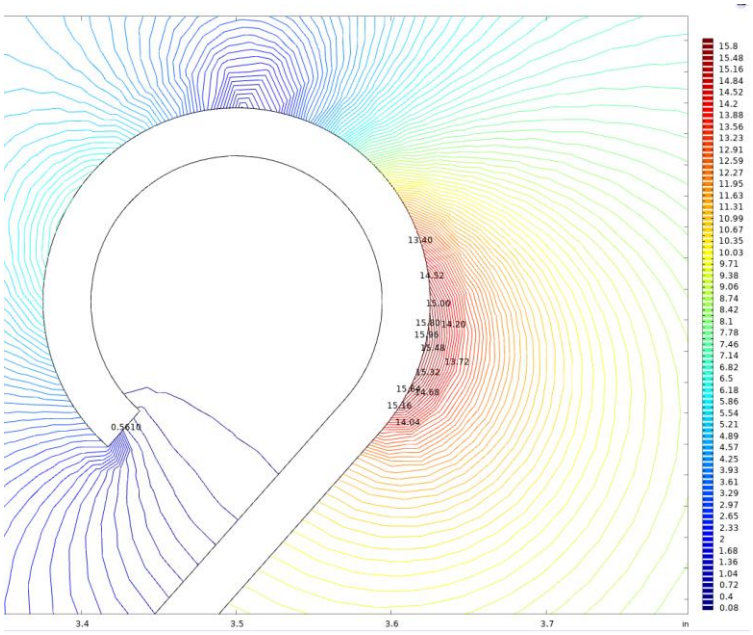

Figure 10: Blow-up view of PHOENIX project second-generation COMSOL model's shroud end hook geometry with electric field lines. Electric field peak of 16 MV/m at the rightmost point of the shroud.

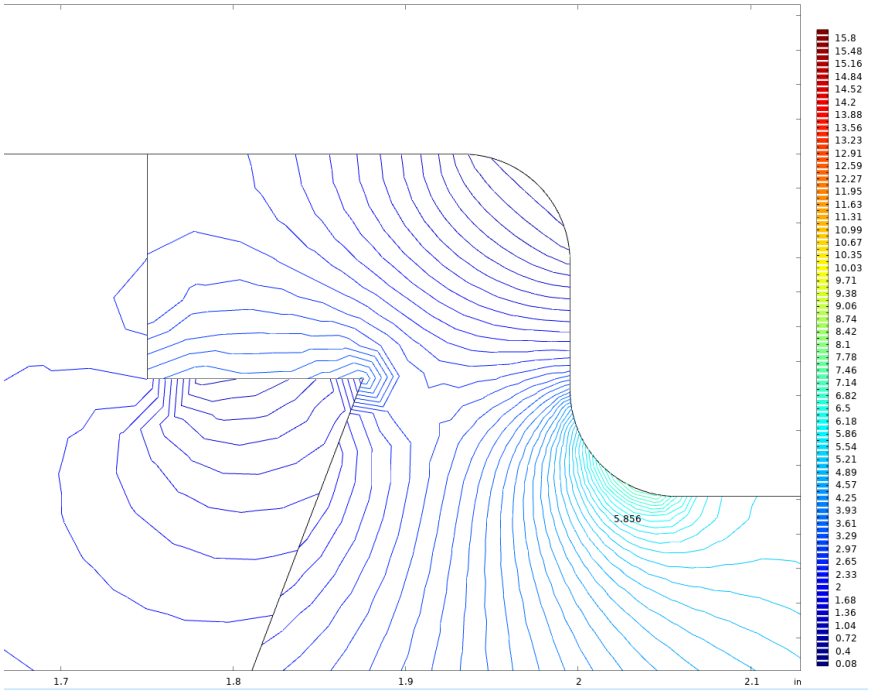

Figure 11: Blow-up view of PHOENIX project second-generation COMSOL model's uppermost triple point with electric field lines. Electric field strength of approximately 3.6 MV/m in this region.

COMSOL Optimized Design

Using the analytic model as a starting point we hand-optimized the various components by carefully shaping the module field shrouds and the Van de Graaff dome to reduce the electric fields. The results of this optimization are shown in Figure 12-17.

In addition, a Pierce-like geometry was included to model the electron gun electrodes including a small, pointed, tungsten-target tip. Somewhat surprisingly, this latter feature was not a strong driver of the peak fields observed thereby giving us some flexibility in the detailed design that will ultimately be fielded.

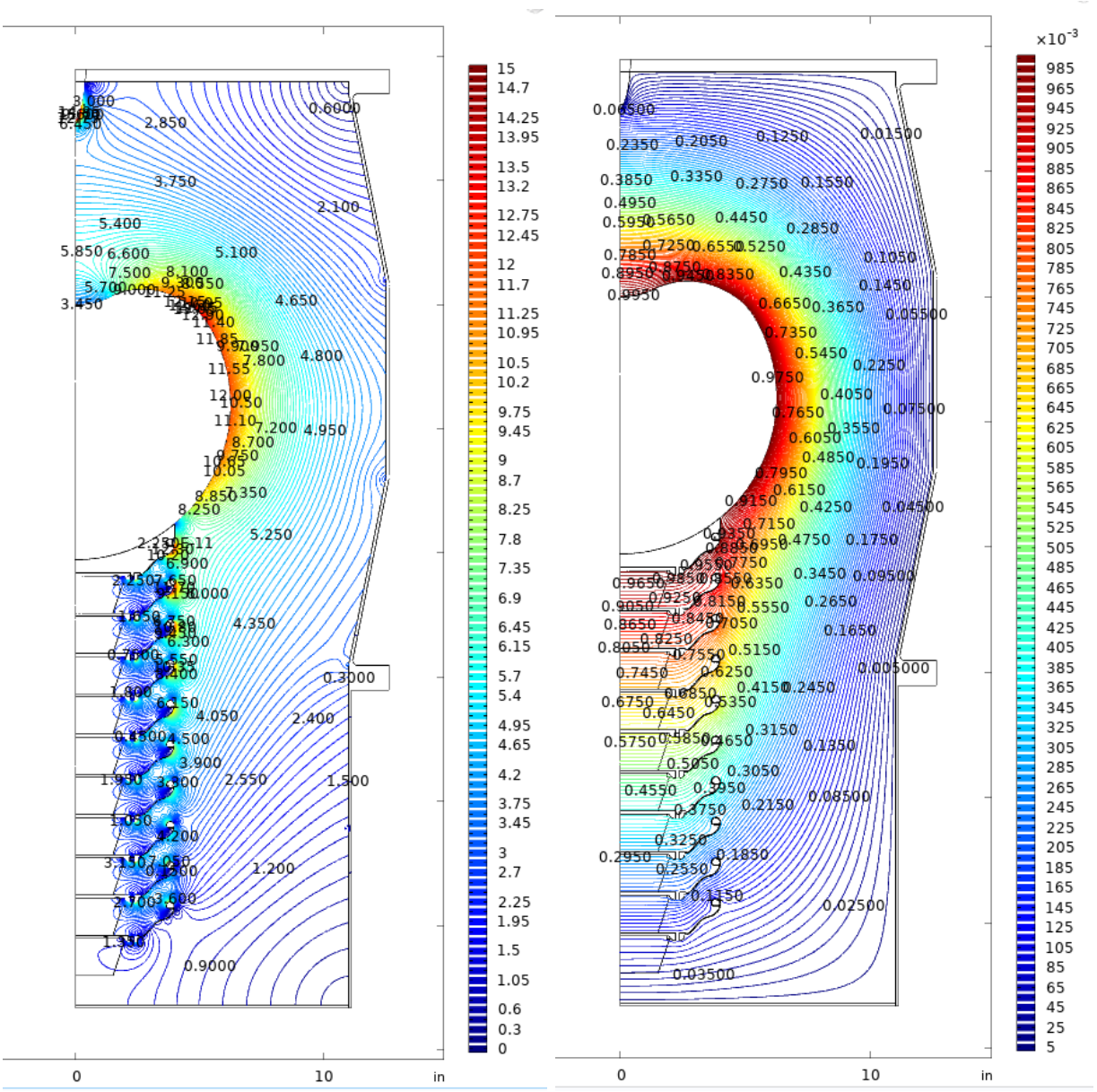

Figure 12: COMSOL optimized model with electric field lines (left) and equipotential lines (right). A peak electric field of 13.2 MV/m was calculated on the Van de Graaff dome.

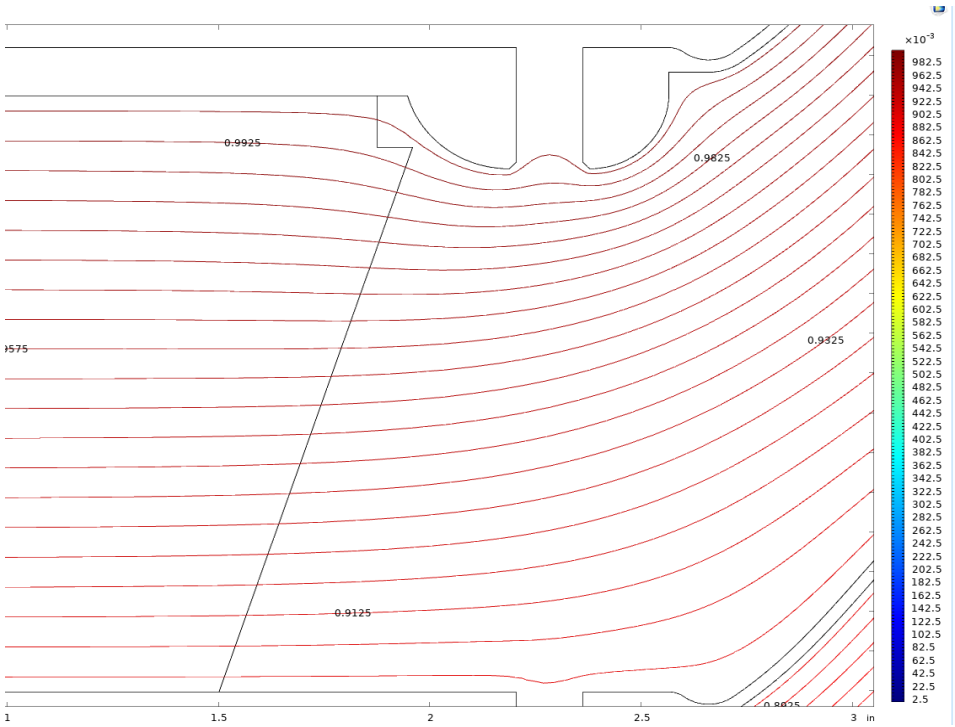

Figure 13: Optimized COMSOL model's cathode-triple-point equipotential lines.

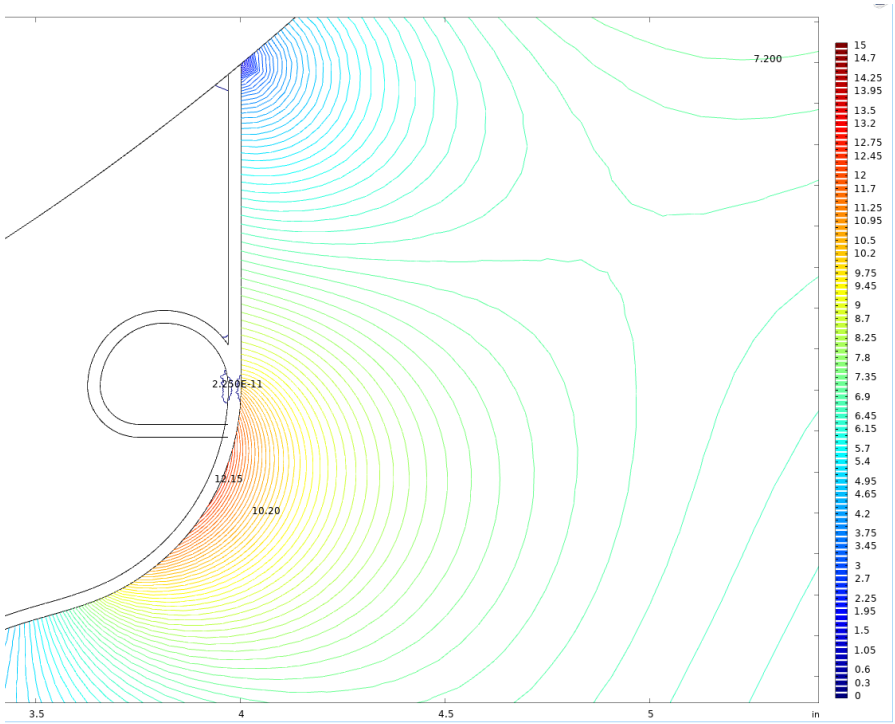

Figure 14: Optimized COMSOL model's welded shroud end hook geometry electric field lines. Electric field peak of 12.3 MV/m on the lower curve of the shroud.

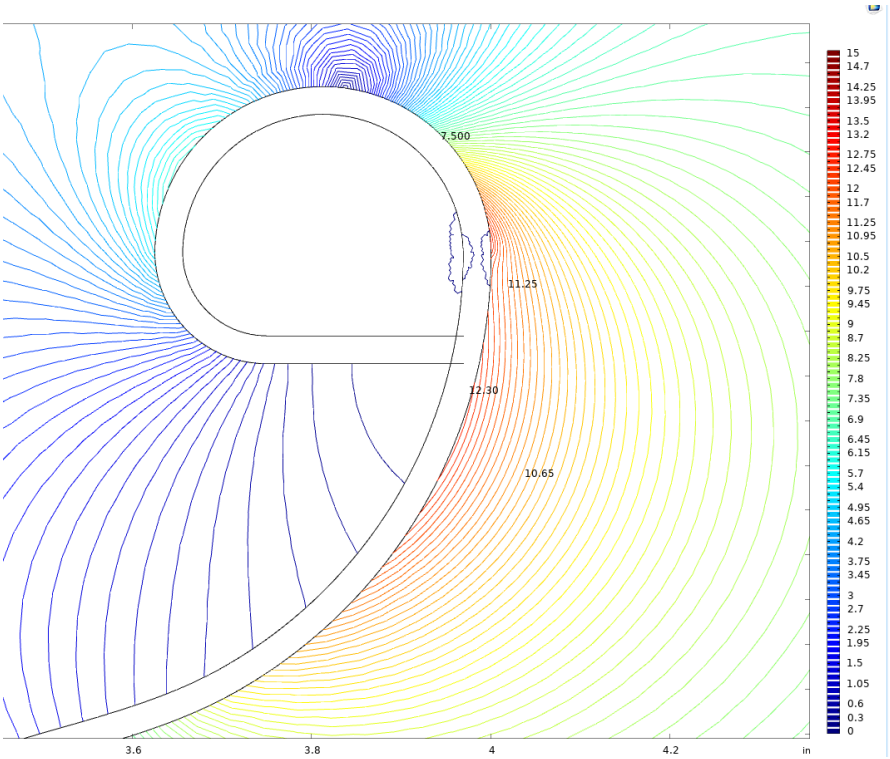

Figure 15: Optimized COMSOL model's shroud end hook geometry with electric field lines. Electric field peak of 12.5 MV/m on the lower curve of the shroud.

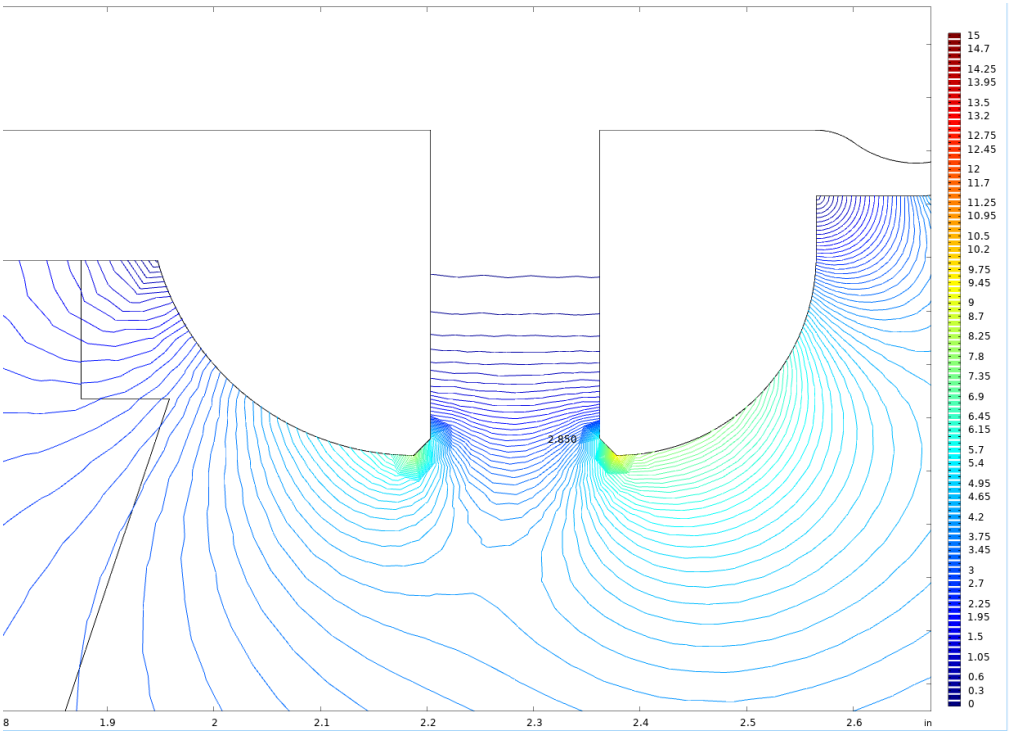

Figure 16: Optimized COMSOL model's shroud plate's bolt-fitting end with electric field lines.

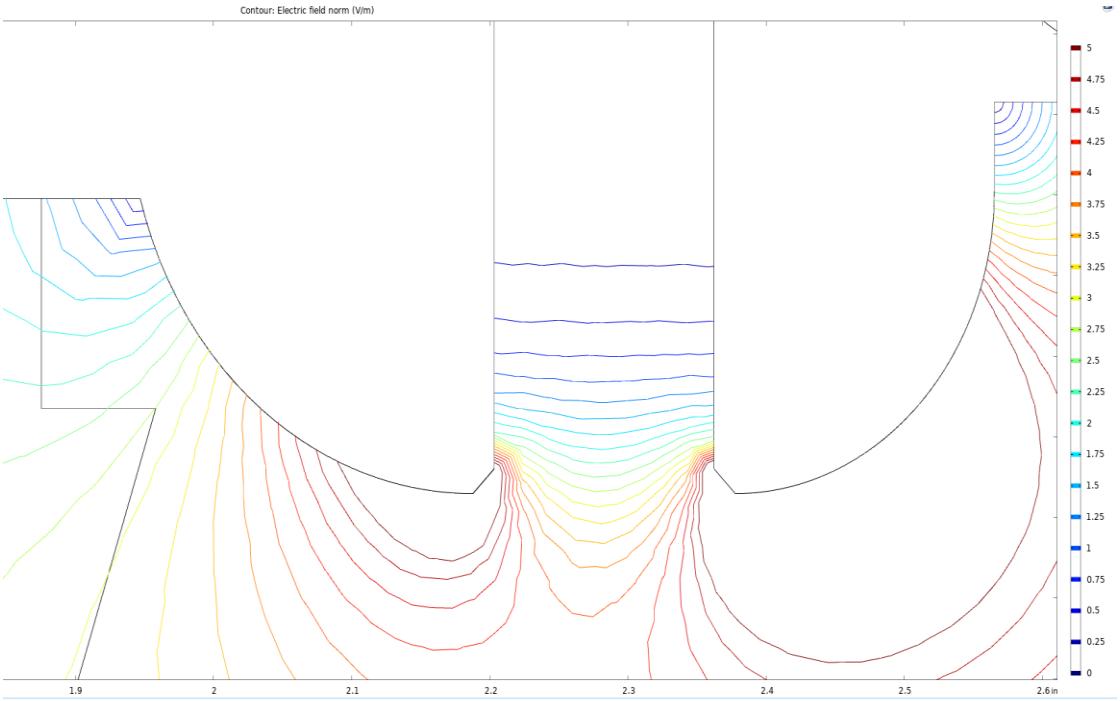

Figure 17: Optimized COMSOL model's cathode-triple-point and surrounding geometry with electric field lines. Electric field strength of approximately 2 MV/m in this region.

One area that needs special attention is the electric field *inside* the Van de Graaff dome. Again, referencing the concentric spheres in Figure 7, if the inner sphere is hollow, and the charge is uniformely distributed on that surface, by symmetry, the electric field at the center of that sphere is zero. However, the magnitude of the electric field on the inner edge of the inner sphere is the same as the field on the outer edge, or, from equation 3:

$$\overrightarrow{E_r} = \frac{Q}{4\pi\varepsilon_o r_i^2} \tag{9}$$

Consequently, if we do nothing to mitigate this field, the polish inside the sphere must be just as good as the polish outside – something that is highly undesireable from a manufacturing perspective. Therefore, we will need to "fill" this sphere with conductors of some type to short-out that adverse electric field, creating, in effect, a (pseudo-)solid sphere.

Conclusions

The COMSOL electic field optimization described herein resulted in substantial reductions in the peak electric fields present in our PHOENIX x-ray diode when operated at a theoretical 1MV on the Van de Graaff dome. The results of these calculations are summarized in Table 1 below. While we fell short of our 10MV/m design goal, the COMSOL optimized design is significantly better than either our prototype or our "back-of-the-envelope" design.

	Electrode Material	Peak Shroud Electric Field	Peak Van de Graaff Dome Electric Field	Typical Cathode Triple Point Field
MFR PHASE I Prototype	Polished Aluminum	30 MV/m (18MV/m)	>30 MV/m	6 MV/m (4MV/m)
PHOENIX Initial Design	Polished Stainless	15 MV/m	16 MV/m	4 MV/m
PHASE II COMSOL Design	Polished Stainless	12.5 MV/m	13.2 MV/m	2 MV/m

Table 1 – Summary of various real and model configurations

Acknowledgements

We would like to thank Carlos Hernandez-Garcia and the photoinjector group at Thomas Jefferson Labs for useful discussions. We are also greatful to Dr. Bill Priedhorsky and the Los Alamos LDRD office and Michael Everhart-Erickson of the Feynman Center For Innovation for ongoing support and IP guidance. Finally we appreciate the programmatic support and encouragement of Chuck Mielke, Mike Steinzig, Dr. Laura Smilowitz, and James Owen of the Los Alamos Weapons Program.

Appendix A – Shroud Drawings

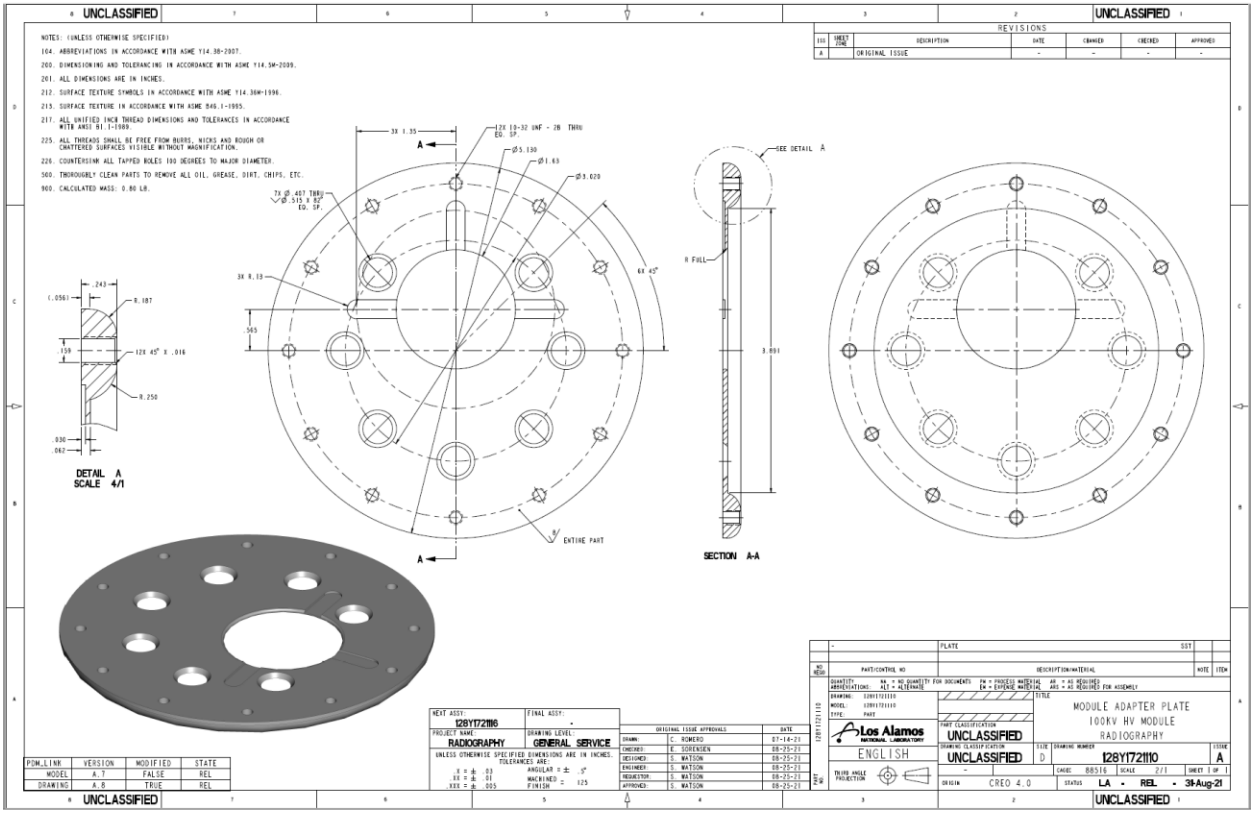

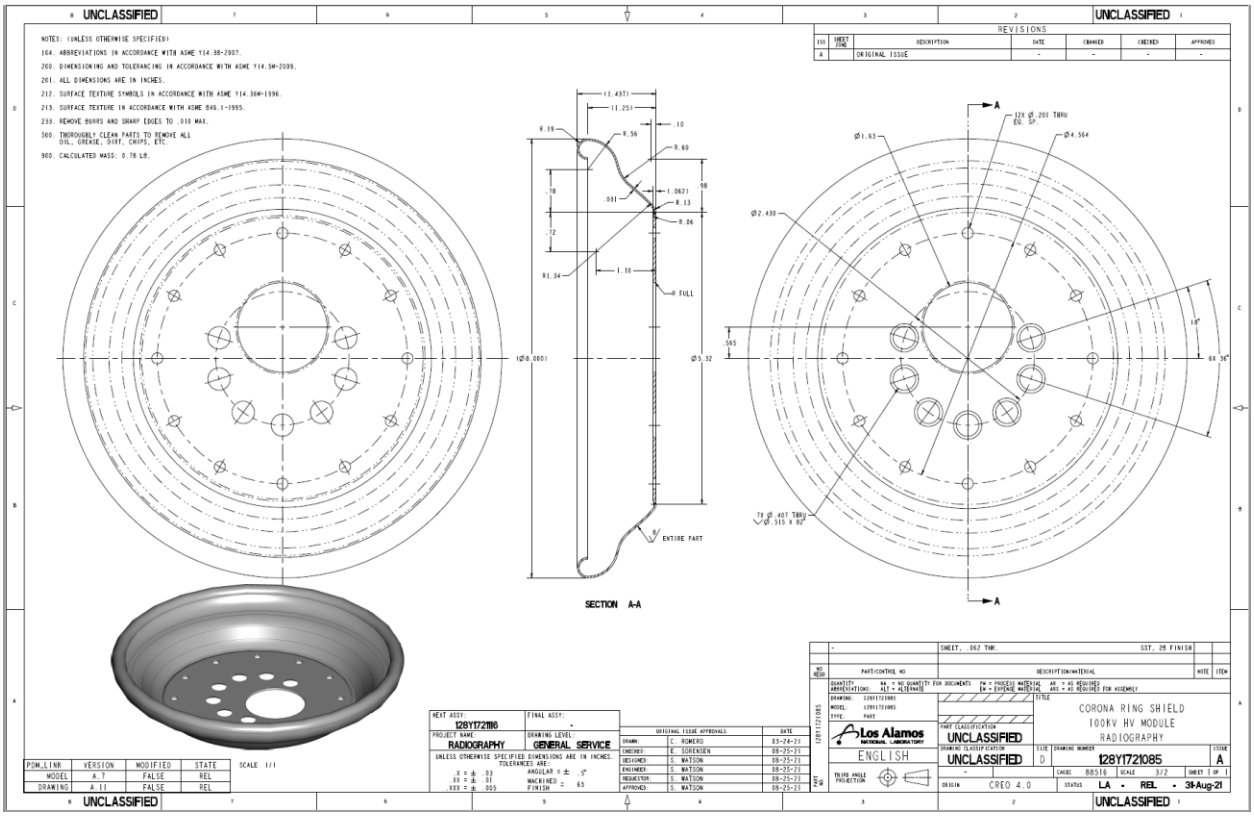

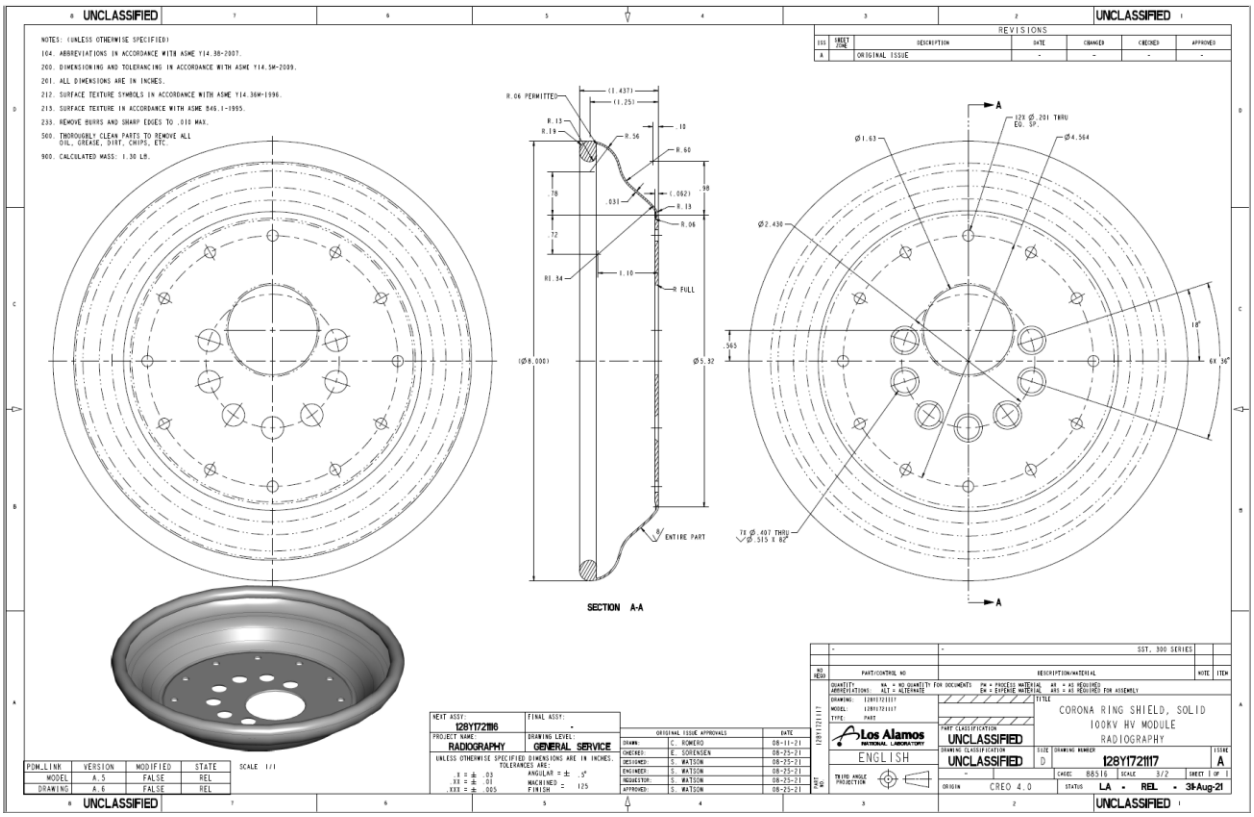
UNCLASSIFIED
NOTES: (UNLESS OTHERWISE SPECIFIED)
104. ABBREVIATIONS IN ACCORDANCE WITH ASME Y14.38-2007.
200. DIMENSIONING AND TOLERANCING IN ACCORDANCE WITH ASME Y14.5M-2009.
201. ALL DIMENSIONS ARE IN INCHES.
212. SURFACE TEXTURE SYMBOLS IN ACCORDANCE WITH ASME Y14.36M-1996.
215. SURFACE TEXTURE IN ACCORDANCE WITH ASME B46.1-1995.
233. REMOVE BURRS AND SHARP EDGES TO .010 MAX.
500. THOROUGHLY CLEAN PARTS TO REMOVE ALL OIL, GREASE, DIRT, CHIPS, ETC.
900. CALCULATED MASS: 1.30 LB.
REVISIONS
A ORIGINAL ISSUE
SECTION A-A
ENTIRE PART
128 Ø.201 THRU EQ. SP.
7X Ø.497 THRU Ø.515 X 82°
SST, 300 SERIES
CORONA RING SHIELD, SOLID
100KV HV MODULE
RADIOGRAPHY
128Y172117
A
UNCLASSIFIED
LA - REL - 31-Aug-21

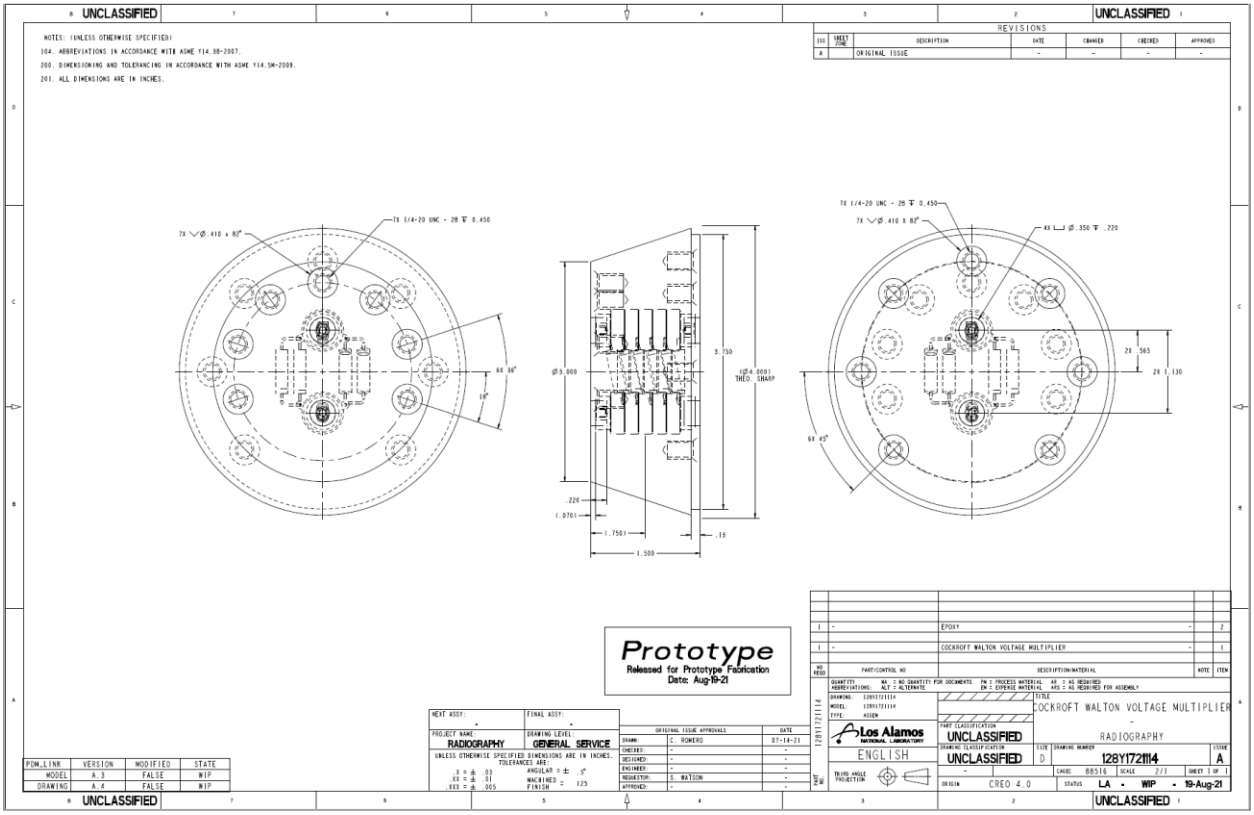
UNCLASSIFIED
NOTES: (UNLESS OTHERWISE SPECIFIED)
104. ABBREVIATIONS IN ACCORDANCE WITH ASME Y14.38-2007.
200. DIMENSIONING AND TOLERANCING IN ACCORDANCE WITH ASME Y14.5M-2009.
201. ALL DIMENSIONS ARE IN INCHES.
REVISIONS
A ORIGINAL ISSUE
7X 1/4-20 UNC - 2B ↧ 0.450
7X Ø.410 x 82°
4X Ø.350 ↧ .220
Prototype
Released for Prototype Fabrication
Date: Aug-19-21
EPOXY
COCKROFT WALTON VOLTAGE MULTIPLIER
COCKROFT WALTON VOLTAGE MULTIPLIER
RADIOGRAPHY
128Y172114
A
UNCLASSIFIED
LA - WIP - 19-Aug-21

References

[1] https://en.wikipedia.org/wiki/Cockcroft%E2%80%93Walton_generator

[2] Benson, S., et al.. *An Inverted Ceramic DC Electron Gun For The Jefferson Laboratory FEL*. Proceedings of FEL 2009. 2009.

[3] Nagai, R., et al.. *High-voltage Testing of a 500kV DC Photocathode Elecron Gun*. Review Of Scientific Instruments. 2010.

[4] Winch, N., & Watson, S.. *Mechanical X-RAY (MEXRAY) Generator For Megavolt Radiography*. IEEE Nuclear Science Symposium. 2018.

[5] Sinclair, C., et al.. Dramatic Reduction of DC Field Emission From Large-Area Electrodes by Plasma-Source Ion Implantation. IEEE Particle Accelerator Conference. 2001.

[6] Abdaullah, M., et al.. Titanium-Nitride Coated Aluminum Electrodes For DC High-Voltage Electron Guns. Journal Of Vacuum Technology. Vol. 33. No. 3. 2015.

[7] Bastani, M., et al.. Evaluation of Niobium As Candidate Elecrode Material For DC High-Voltage Photoelectron Guns. Physical Review Special Topics – Accelerators and Beams. 2012.

[8] Zhang, Y., et al.. Micro-effect of Surface Polishing Treatment on Microscopic Field-Enhancement and Long vacuum Gap Breakdown. AIP Advances. 2016.

[9] https://www.comsol.com/